PHYSICAL REVIEW D **92,** 014015 (2015)

Probe Higgs boson pair production via the $3\ell 2j + \not{E}$ mode

Qiang Li,[1,2] Zhao Li,[3] Qi-Shu Yan,[2,4,5] and Xiaoran Zhao[3,4,*]

[1]*Department of Physics and State Key Laboratory of Nuclear Physics and Technology, Peking University, Beijing 100871, China*

[2]*CAS Center for Excellence in Particle Physics, Beijing 100049, China*

[3]*Institute of High Energy Physics, Chinese Academy of Sciences, Beijing 100049, People's Republic of China*

[4]*School of Physics Sciences, University of Chinese Academy of Sciences, Beijing 100049, People's Republic of China*

[5]*Center for High-Energy Physics, Peking University, Beijing 100871, People's Republic of China*

(Received 2 May 2015; published 13 July 2015)

We perform a detailed hadron-level study on the sensitivity of Higgs boson pair production via the WW^*WW^* channel with the final state $3\ell 2j + \not{E}$ at the LHC with the collision energy $\sqrt{S} = 14$ TeV and a future 100 TeV collider. To avoid the huge background from $pp \to ZW +$ jet processes, we confine to consider the four-lepton patterns: $e^{\pm}e^{\pm}\mu^{\mp}$ and $\mu^{\pm}\mu^{\pm}e^{\mp}$. We propose a partial reconstruction method to determine the most reliable combination. After that, we examine a few crucial observables which can efficiently discriminate signal and background events, especially we notice that the observable m_{T2} is very efficient. For the LHC 14 TeV collisions, with an accumulated 3000 fb^{-1} data set, we find that the sensitivity of this mode can reach up to 1.5σ for the Standard Model and the triple coupling of Higgs boson λ_3 in the simplest effective theory can be constrained into the range $[-1, 8]$ at 95% confidence level; at a 100 TeV collider with the integrated luminosity 3000 fb^{-1}, the sensitivity can reach up to 13σ for the Standard Model and we find that all values of λ_3 in the effective theory can be covered up to 3σ even without optimizing signals. To precisely measure the triple coupling of Higgs boson $\lambda_3 = 1$ of the Standard Model at a 100 TeV collider, by using the invariant mass of three leptons which is robust against the contamination of underlying events and pileup effects and by performing a χ^2 analysis, we find that it can be determined into a range [0.8, 1.5] at 95% confidence level.

DOI: 10.1103/PhysRevD.92.014015 PACS numbers: 13.85.Qk, 14.80.Bn

I. INTRODUCTION

The last building block of the Standard Model (SM), Higgs boson, has been discovered by ATLAS and CMS collaborations [1,2]. The interaction of Higgs boson with the fermions of the SM and its self-couplings are new types of interactions which are different from those described by the gauge symmetries in the SM. To ascertain the nature of Higgs boson, it is important to precisely measure the Yukawa-type interactions which can be determined by measuring the Higgs decay into fermion pairs from single Higgs production at future LHC runs and Higgs factories [3,4], while the analysis on the Higgs self-couplings via Higgs pair and multi-Higgs boson production is achievable at high luminosity LHC runs and future pp collider, say a 100 TeV collider [5].

The determination of the Higgs potential is of important significance, since the potential is directly related to the structure of vacuum, the electroweak phase transition and electroweak baryogenesis, and the fate of our Universe as well. It is useful to address the issue whether the Higgs boson is elementary or composite. It is also crucial to probe new physics, which is believed to exist somewhere and somehow since there are fundamental issues which cannot be solved by the SM itself, e.g., the matter-antimatter asymmetry in our Universe, the quadratic divergence of the Higgs mass term, and the mystery of dark matter, etc.

The SM predicts trilinear and quartic self-couplings in the Higgs potential at tree level. Both trilinear and quartic Higgs self-couplings are related to the Higgs boson mass by $m_H^2 = \frac{1}{2}\lambda_{\mathrm{SM}}v^2$, where trilinear and quartic couplings are proportional to λ_{SM}, which is the dimensionless coupling of Higgs potential before electroweak symmetry breaking. In the language of an effective field theory, the trilinear coupling term can be simply expressed as

$$L = \frac{\lambda_3}{6}\lambda_{\mathrm{SM}}^{\mathrm{tr}} v H^3 = \lambda_3 \frac{\lambda_{\mathrm{SM}}}{4} v H^3, \tag{1}$$

where $\lambda_3 = 1$ corresponds to the SM case and there is a relation $\lambda_{\mathrm{SM}}^{\mathrm{tr}} = 3/2\lambda_{\mathrm{SM}}$ in this parametrization. It is well known that to determine the quartic coupling of the SM might be challenging at the LHC due to the small production rate of three Higgs boson final state, but to detect the trilinear coupling via Higgs pair production is expected to be within the reach of the LHC. The measure of

*zhaoxiaoran13@mails.ucas.ac.cn

the trilinear coupling up to the precision 10% at a future 100 TeV colliders is feasible [6], which can further pinpoint and discover new physics.

The importance of Higgs pair production has attracted attention a long time ago. Theoretical investigations on the Higgs pair production in the SM began with the pioneering works [7–9], where the gluon-gluon fusion [7] and the vector boson fusion [8,9] processes had been considered. It has been found that at hadron colliders the gluon-gluon fusion production is almost 1 order of magnitude larger than the weak boson fusion process. There are lots of efforts to improve theoretical prediction on the Higgs pair production. For example, the next-to-leading order (NLO) and next-to-next-to-leading order (NNLO) QCD corrections to gluon-gluon fusion had been considered in [10,11] and recently in [12] by using the large top mass approximation and normalizing the partonic cross section using the exact LO result. The finite top quark mass effects have been analyzed at NLO in [13] via expansion by top quark mass. Recently, NNLO QCD corrections to the vector boson fusion Higgs pair production has been done by the USTC group [14].

Besides detecting the Higgs self-couplings of the SM, multi-Higgs production at various colliders is of great importance to probe new physics, as explored in Ref. [15]. At hadron colliders, Higgs pairs can be enhanced by other heavier scalar resonances [16–20]. By measuring the signal of Higgs pair production, we can extract the triple Higgs coupling and then depict the shape of the Higgs potential so as to distinguish various electroweak symmetry breaking models. For example, the composite models predict a vanishing or small triple couplings [21] and a model with effective potential $V = \lambda(H^+H)^2 + (H^+H)^3/\Lambda^2$ predicts a triple Higgs coupling $7/3$ times that of the SM. The measurement of the cross section of Higgs pair production is also important to distinguish models where Higgs is assumed to be elementary, like in the supersymmetric model where superparticles can enhance the production rate [22–24] and like in the two-Higgs doublet model the extra scalars can enhance the production rate [25], while the Higgs-gravity model [26,27] predicts a coupling dependent of external momenta. These specific models can be more generally formulated and conveniently explored in the framework of the effective Lagrangian up to $O(p^6)$ [28], as demonstrated in a recent study in Ref. [29].

A comprehensive study on various productions at the generator level has been recently investigated in [30] by using the automatic matrix element generator MADGRAPH5. According to the study of [30], in the SM the leading contribution to Higgs pair production at the LHC and a future 100 TeV collider is via gluon-gluon fusion. The subleading production mechanism is via weak vector boson fusion processes [14,31]. The $t\bar{t}$ associated production can become comparable with the weak vector boson fusion production when the collision energy is around 100 TeV [30]. The effects of top quark mass in double and triple Higgs production at hadron colliders have been studied in [32]. The kinematics of the di-Higgs bosons decay to $b\bar{b}\gamma\gamma$ have been analyzed in [33] and their effects to the measurement of nonstandard values of λ_3 have been explored. Interested readers can refer to [34,35] for theoretical progress in the fixed order QCD calculation for single Higgs and Higgs pair productions, and top quark pair production as well.

Except the theoretical efforts on the Higgs pair production, there are lots of efforts to improve theoretical predictions of the Higgs boson decay. For a Higgs boson with mass around 125–126 GeV, its main decay final state is $b\bar{b}$, and the state-of-art research on its partial width is up to $O(\alpha_S^4)$ in [36]. Higgs decaying into other fermion pairs has also been investigated up to the two loop level. The $H \to gg$ decay channel is up to N^{3}LO QCD in [37] in the large top quark mass limit, and the top quark mass effects are analyzed in [38]. The partial width of $H \to \gamma\gamma$ channel is known up to NLO EW and NNLO QCD [39,40]. The decay channel $H \to Z\gamma$ is known up to NLO QCD in [41]. For the decay channel $H \to WW^*, ZZ^* \to 4f$, $O(\alpha_S)$ and $O(\alpha)$ corrections have been studied in [42–44]. Interested readers can refer to [45–49] for more information on the current status of our understanding of Higgs boson.

Recently the signals of Higgs boson pair production at the LHC have been further studied via a few decay channels. A recent theoretical review can be found in [31,50]. For example, the study of the $HH \to b\bar{b}\gamma\gamma$ channel can be found in Ref. [51] with a significance of about 1.5σ for an integrated luminosity 600 fb^{-1} at LHC with 14 TeV collision energy is assumed. A recent search by the CMS collaborations can be found in Ref. [52]. The authors of Ref. [31] updated this study and provided a significance of about 6.46σ for the integrated luminosity 3000 fb^{-1} at 14 TeV. The study for the $HH \to b\bar{b}\tau^+\tau^-$ channel can be found in Refs. [31,53,54], where the authors of Ref. [31] provided a significance of about 9.36σ for 3000 fb^{-1} LHC. The channel $HH \to b\bar{b}W^+W^- \to b\bar{b}\ell\nu_\ell jj$ has been studied in Ref. [55], where a significance of 3.1σ for 600 fb^{-1} LHC has been obtained. The mode $HH \to b\bar{b}W^+W^- \to b\bar{b}\ell\nu_\ell\ell'\nu_{\ell'}$ has been studied in Ref. [31] and a significance of about 1.53σ for 3000 fb^{-1} the LHC has been achieved. A recent updated study on 4 b jet final state can be found in Ref. [56] and a search for new physics by the CMS collaborations can be found in Ref. [57]. The probe of the vector boson fusion Higgs pair production can be found in Ref. [58]. The associated production $t\bar{t}hh$ of the final states $t\bar{t}bbbb$ has been studied in Ref. [59].

The third largest decay fraction channel for Higgs pair is the WW^*WW^* channel. The subsequent decay mode $8j$ and $l6j + \not{E}$ will be too hard to be found due to huge QCD multijets and W + multijets background. The decay mode $l^\pm l^\mp 4j + \not{E}$ will be also too hard to be found due to the huge $Z(\gamma^*)$ + multijets and W^+W^- + multijets background. The decay mode $4l+$ missing energy will have

a tiny production rate. So only two subsequent decay channels are reachable: two same-signed lepton mode $l^{\pm}l^{\pm}4j+\not{E}$ and three leptons mode $3\ell 2j+\not{E}$.

These channels had been taken into account in Refs. [60,61] with the assumption that the Higgs mass is in the range 140 GeV $< m_H <$ 200 GeV and the WW is the main decay channel for Higgs and both W bosons are on shell, where, at parton level, important acceptance cuts and some simple kinematic variables, especially the invariant mass of all final states which was crucial to suppress the background events of $t\bar{t}+$ jets and multitop processes, were carefully studied. Considering that the measured Higgs boson mass is 125 GeV or so and the branching fraction of Higgs boson decay to WW^* is considerably smaller than that assumption in Refs. [60,61], the production rate of the signal in this final state is almost 1 order of magnitude smaller and the discovery of the signal in this mode is very challenging. Furthermore, not all the W bosons from the decay of Higgs boson can be on shell which makes the signal hard to be distinguished. Therefore it is necessary and quite nontrivial to revisit and perform a more detailed analysis by taking all these facts into account. In this paper, we propose a partial reconstruction procedure of the Higgs pair in the final states and examine more useful kinematic variables especially the m_{T2} variable in our analysis, which has been found can suppress most of the background efficiently. In order to further improve the significance, we also apply two multivariate analysis approaches to optimize the signal and background discrimination.

In this paper, we update the study explored in Ref. [61] and consider the $3l2j+\not{E}$ final state in more detail and will focus on the sensitivity at the LHC and a future 100 TeV collider to the triple Higgs coupling. It is confirmed that the background from $ZW+$ jets is huge. In order to overcome this type of background, we deliberately consider the four three-lepton patterns: $e^{\pm}e^{\pm}\mu^{\mp}$ and $\mu^{\pm}\mu^{\pm}e^{\mp}$. Since it is essential to reconstruct the crucial information of signal events, we propose a partial reconstruction method and an efficient method to find the right combination of Higgs bosons. After the reconstruction, we further construct most of the kinematical variables, especially the m_{T2} observable and examine their discrimination power to signal and background events. Considering the signal events are few, in order to enhance the significance, we apply two multivariate analysis methods to optimize the signal and background discrimination. Our results show that this channel can reach a sensible significance, i.e., 1.5 or so, at the 14 TeV LHC with 3000 fb^{-1} of integrated luminosity. We also extend the study to 100 TeV collisions with a luminosity 3 ab^{-1} and find that the mode can be used to explore the discovery of all values of λ_3. When the SM will be confirmed, this mode can also be used to perform precision measure of λ_3 to the range [0.8, 1.5], which is comparable with the precision measurement by using the ratio of cross sections as pointed out in [62].

This work is organized as follows. We will describe the event generation of signal and background in Sec. II. Due to the existence of three neutrinos which consist of missing energy in events and are unable to be fully reconstructed, we will propose a partial reconstruction method for the visible objects and analyze the key kinematic features of signal events in the $3l2j+\not{E}$ mode in Sec. II. By using the constructed kinematic observables, we will consider the sensitivity of 14 TeV LHC and a 100 TeV collider in Sec. IV. We will end this paper with discussions and conclusions.

II. EVENT GENERATION AND KINEMATIC FEATURES OF SIGNAL EVENTS

We have generated the signal events in the following steps. (1) We have used the leading order matrix element computed by MadLoop/aMC@NLO [63] and Gosam [64], which have taken into account the top-quark mass dependence in the loop evaluations. We have cross-checked the generated codes with the matrix element obtained by the FormCalc [65], and have found these independent approaches yielding the same results. (2) We perform the integration over the whole phase space by using the vbfnlo code [66–68] and obtain the total cross section. (3) After reaching a stable total cross section to the desired precision, we reweight each event in the phase space so as to yield the unweighted events at the parton level.

For the LO cross sections, we used CTEQ6L1 [69] PDF sets. We set the cuts in the phase space for the final Higgs bosons as $|\eta(H)|<5$ and $P_t(H) > 1$ GeV. We set the renormalization and factorization scales as $\mu_r=\mu_f=\sqrt{\hat{s}}$, and have reproduced the LO total cross section as 22.8 fb, which agrees with our previous results [70].

Using the unweighted events, we use the package decay provided in MadGraph5 [71] to decay Higgs into a pair of W bosons (one is on shell and the other is of shell) and further to decay W bosons into quarks and leptons. Therefore, all spin correlation information in the final states has been taken into account in the data sample. Before considering lepton and jet and missing energy reconstruction at detector level, we use pythia6 [72] to perform parton showering.

For the background processes, we use MadGraph5 [71] to generate events, and also shower it with pythia6 [72]. In order to avoid the double-counting issue of jets originated from matrix element calculation and the parton shower, we apply the MLM matching [73] implemented in MadGraph5 [71]. In practice, for the background events of $t\bar{t}W$, we include both processes $pp\to t\bar{t}W$ and $pp\to t\bar{t}W+j$ to form an inclusive data set. For the background events of WWW, we include processes $pp\to WWW$ and $pp\to WWW+j$ and $pp\to WWW+jj$, and similarly for ZW,HW backgrounds. The $ZW^{\pm}\to l^+l^-W$ backgrounds are generated by using exact matrix element which include off-shell Z and γ effects, and other backgrounds are all

generated on mass shell. We ignore the ZZ background because it requires one lepton is missing and should be much smaller than the ZW background. The background $t\bar{t}Z$,ZWW is also ignored because it is much (20–30 times) smaller compared to the $t\bar{t}W$,WWW background, correspondingly. We also ignore $t\bar{t}t\bar{t}$ due to its tiny cross section and the efficient rejection by b-taggings. We would like to mention that in all background event generation the decay

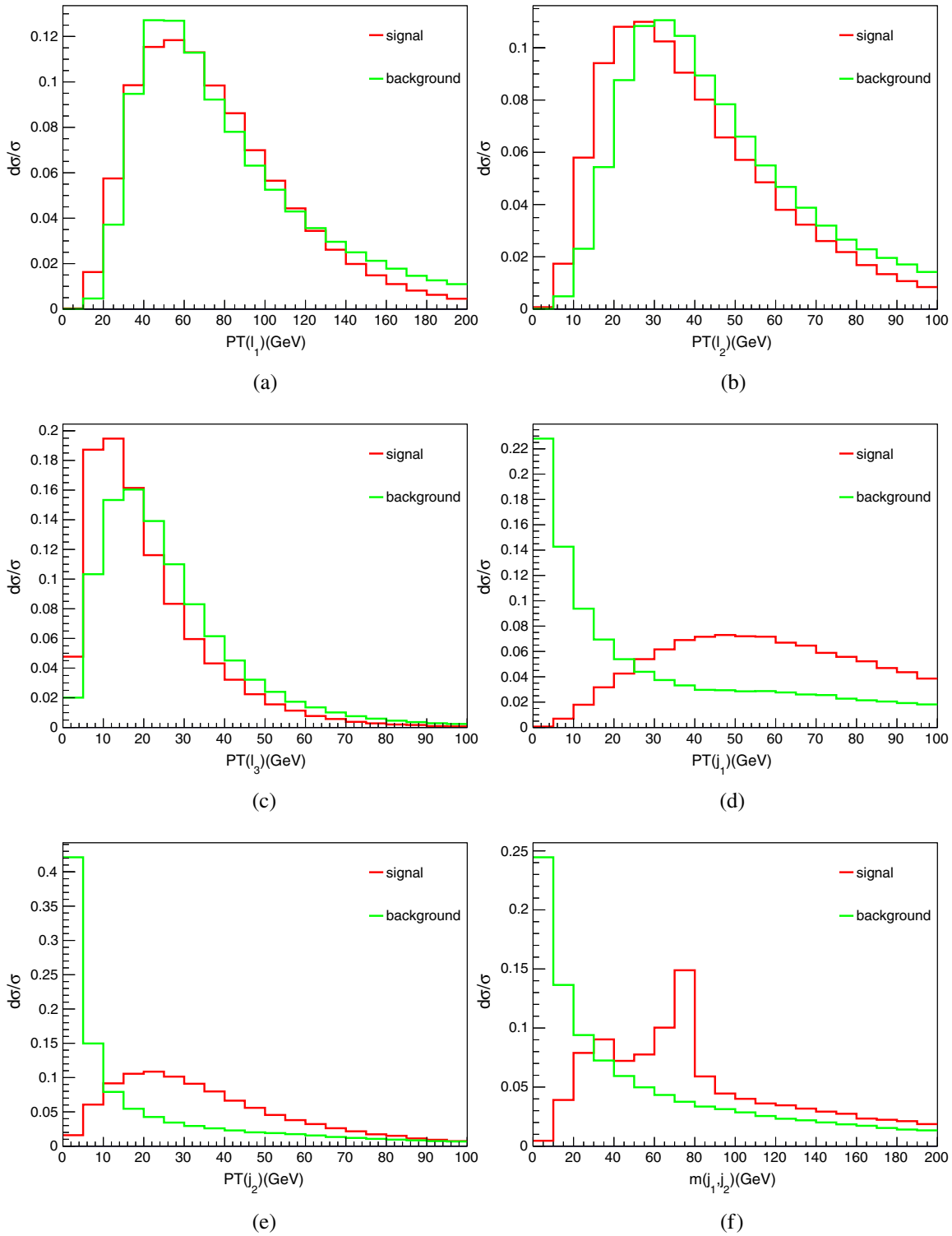

FIG. 1 (color online). The transverse momentum of leading three leptons and leading two jets and the invariant mass of two jets as well are shown at parton level. Both signal and background are normalized one. (a) P_t of 1st lepton; (b) $P_t$of 2nd lepton; (c) P_t of 3rd lepton; (d) P_t of 1st Jet; (e) P_t of 2nd Jet; (f) Invariant mass of two leading jets.

correlation for all final states has been correctly accounted for.

For the analysis at the detector level, we first reconstruct isolated leptons in each event. After that we pass all of the rest of the visible particles to FastJet [74] to cluster into jets. We adopt the anti-kt algorithm [75] with cone parameter $R = 0.4$. After that, the transverse missing energy is reconstructed. In this study, we have neither taken into account the magnetic effects for charged tracks nor the energy smearing effects for leptons and jets. Therefore, our analysis should be regarded as a hadron level analysis.

In order to suppress the dominant background and select the most relevant events, we introduce all of the following preselection cuts at the event-by-event level:

(i) We veto events with isolated and energetic photon(s) with $P_t(\gamma) > 10$ GeV and $|\eta(\gamma)| < 2.5$.

(ii) In order to suppress the large background from $t\bar{t}W$ and $t\bar{t}H$, we veto events with tagged B jets. In our simulation, the tagging efficiency of B jets is assumed 60%. Therefore, roughly the background from $t\bar{t}W$ and $t\bar{t}H$ can be suppressed by a factor 0.16.

(iii) The preselection rule for three isolated leptons is found to be crucial. We demand that there are exactly three isolated leptons being found, with the requirement that the first leading lepton should have a momentum larger than 30 GeV, the next leading lepton should be larger than 10 GeV, and the softest lepton should be larger than 10 GeV. Since there must be a lepton coming from the on-shell W boson decay, we require the leading lepton should be hard enough. In the meantime, there must be a softer lepton which comes from off-shell W boson decay. In order to increase the acceptance for signal, we deliberately lower the momentum of the third lepton. In Figs. 1(a)–(c), we present the distributions of three leptons. Considering that the threshold of lepton reconstruction is around 3 GeV and if the lepton is larger than 5–8 GeV at both CMS and ATLAS detectors lepton reconstruction efficiency can be 95% [76,77], to find the soft leptons with $P_t > 10$ GeV in the signal event should be plausible.

(iv) In order to suppress the large background $Z/\gamma W + \mathrm{jj}$, we only consider the following four modes with two leptons of same sign and same flavor plus an extra different flavored lepton: $e^-e^-\mu^+$, $e^+e^+\mu^-$, $\mu^+\mu^+e^-$, and $\mu^-\mu^-e^+$. After this preselection cut, we noticed that the background events from the processes $Z/\gamma W + \mathrm{jj}$ can be safely neglected.

(v) At least two jets in the events are required to be successfully reconstructed, i.e., $n_j \geq 2$ and $|\eta(j)| < 2.5$. Among those reconstructed jets, there are two jets which could come from a W boson either on shell or off shell. In order to increase the acceptance of signal, we only consider those jets with transverse momentum larger than 15 GeV. We show the distributions of these two leading jet in Figs. 1(d) and 1(e). We also show the invariant mass of these two jets in Fig. 1(f). It is noticed that the invariant mass in signal events can produce two peaks, one is near the value of M_W and the other is near that of $M_H - M_W$.

(vi) The missing transverse momentum is required to be larger than $\not{E}_T > 20$ GeV due to neutrinos in the signal processes. The requirement on large missing energy is also useful in order to suppress the huge QCD processes and to save the computing time.

The LHC detectors can record signal events, which can be triggered by both energetic charged lepton and large missing energy. From Table I, we observe that the number of background events is around 200 times larger than that of signal events, and it is indeed a challenge if we want to distinguish the signal and the background successfully.

In order to distinguish the signal and background event, we have to resort to the reconstruction procedure so as to extract the most important information of signal. Since the Higgs boson is a neutral particle, for the decay mode $\ell_1^\pm\ell_2^\pm\ell_3^\mp 2j + E$, without considering the neutrinos, there are only two possible combinations for a pair of Higgs boson decay: $(H(\ell_1^\pm\ell_3^\mp), H(\ell_2^\pm jj))$ or $(H(\ell_2^\pm\ell_3^\mp), H(\ell_1^\pm jj))$. For the convenience of later study, hereby we label the first

TABLE I. The number of signal and background events are shown. Here we assume the total integrated luminosity as 3 ab^{-1}.

Processes	$\sigma^{\mathrm{LO}} \times$ branching fraction (fb)	K factors	No. events after preselection cuts
Signal $gg \to HH$	3.0×10^{-2}	1.8 [12]	13.7
$HW^\pm$	1.2	1.2 [78]	94.4
WWW	1.4	1.8 [79]	400.6
$\mathrm{t\bar{t}}W^\pm$	4.6	1.3 [80]	317.2
$\mathrm{t\bar{t}}H$	2.1	1.2 [81]	101.3
$ZW, \gamma W$	233	1.8 [82]	~0
S/B		0.015	
$S/\sqrt{B}$		0.45	

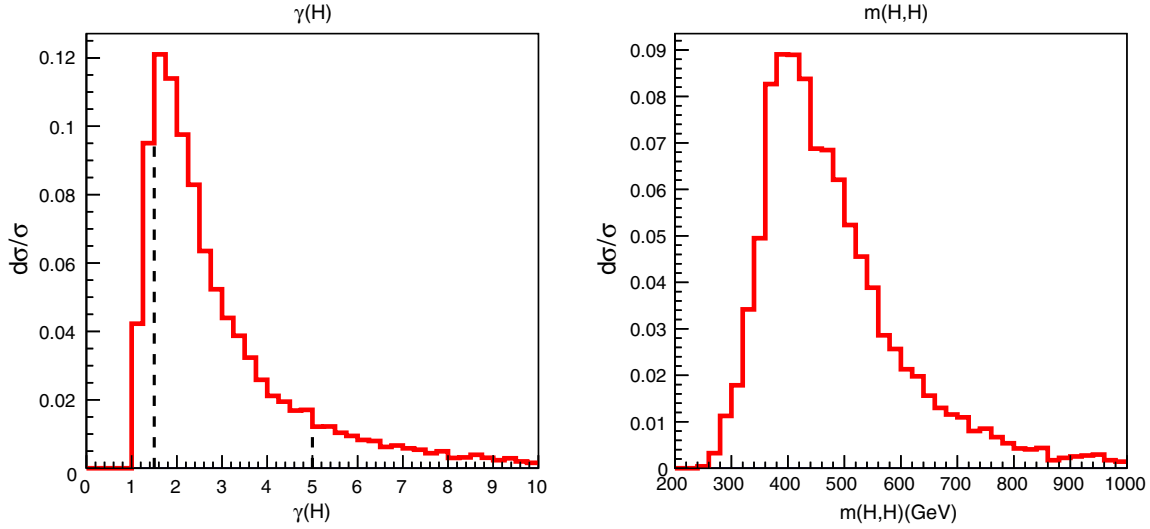

FIG. 2 (color online). The γ factor [$\gamma = E(H)/m_H$] and the invariant mass of Higgs pair are shown at the parton level.

Higgs boson as a leptonic one [$H(\ell\ell)$] and the second one as a semileptonic one [$H(\ell jj)$].

As we can read from the left panel of Fig. 2, each of the Higgs bosons is moderately boosted when produced and the peak value of γ [here γ is defined as $E(H)/m_H$, which is a measure to the boost] is around 2. The fraction of highly boosted Higgs boson $\gamma > 5$ is around 13% or so, while the fraction of moderately boosted Higgs boson $\gamma > 1.5$ is around 87%. In the right panel of Fig. 2, we show the invariant mass of the Higgs pair. It is observed that the peak region of the invariant mass of Higgs pair is around 360–540 GeV, which explains why most of the Higgs pairs are boosted.

III. RECONSTRUCTION OF SIGNAL AND OBSERVABLES

To know the right combination is crucial to reconstruct the kinematic features of the signal and can provide important information to suppress background events. For that purpose, we need to find a way to determine the right combination reliably.

A. Determination of the right combination

Fortunately, the problem at hand is not complicated after the preselection and the number of combinations is not formidable. It is observed that in the selected events, there are three leptons in total. Two leptons with the same sign and the same flavor must come from different Higgs bosons, there are only two possible combinations for each signal event. The remaining task is to find the right combination by exploiting the kinematics of Higgs bosons.

Keeping those kinematic features of Higgs bosons in signal events exposed in the last section, we consider the following six individual methods by using different observables to pick out the combination from two as a solution for each event. In Table II, we tabulate the principal observables and the percentage of correctness to pick out the right combinations at parton level, which serves as an important guide for our later analysis at the hadronic/detector level. Below, we examine the efficiency of these six methods one by one.

(1) In the first method, we utilize the fact that the mass of the Higgs bosons in the pair production must be the same. But due to the missing energy carried away by the neutrinos, if we use the condition that the mass difference should be smaller we find that we can only reach the right combination in 69%.

(2) In the second method, we use the fact that most of the Higgs bosons are moderately boosted and two leptons from the leptonic Higgs are tended to be close in spatial separation due to the spin correlation of W bosons from Higgs decay [83,84], therefore two leptons from its decay should have a smaller angle separation $\Delta R(\ell^+, \ell^-)$. We notice that by using this observable, the right combination can be determined by 85%.

(3) In the third method, we use the semileptonic Higgs as a guide by requiring the smaller angle separation

TABLE II. The principal observables to choose the right combination in six methods and the percentage of correctness at the parton level are tabulated.

Methods	The percentage of correctness (%)
$\lvert m_{H(ll)} - m_{H(ljj)}\rvert$	68.9
$\Delta R(l^{\pm}, l^{\mp})$	85.0
$\Delta R(l^{\pm}, W_{jj})$	89.9
$P_t[H(ll)] + P_t[H(ljj)]$	90.3
$\Delta_R(H(ll), H(ljj))$	92.0
$m_{H(ll)} + m_{H(ljj)}$	95.4

$\Delta R(\ell, W_{jj})$ between a lepton and a hadronic W. Due to the smaller energy loss from its decay, we observe a higher percentage in choosing the right combination when compared with the second method, which can reach to 90%.

(4) In the fourth method, we resort to the scalar sum of the transverse momenta of Higgs pair (without taking into account the missing transverse momentum), which should be large due to the energy conservation in the transverse direction. When the wrong combination is made, the scalar sum is found to decrease. The method can have similar performance as the third method.

(5) In the fifth method, we exploit the fact that two Higgs bosons mostly fly back to back in 3d space, therefore the angular separation of them, $\Delta R(H(\ell\ell), H(\ell jj)) = \sqrt{\Delta\phi^2 + \Delta\eta^2}$, should be large. For the two possible combinations, we choose the one which yields the larger $\Delta R(H(\ell\ell), H(\ell jj))$ as the solution and we observe that this method can arrive at an efficiency 92%.

(6) In the sixth method, we compute the invariant mass of each Higgs boson from visible objects, which can be labeled as $m_{H(\ell\ell)}$ and $m_{H(\ell jj)}$, respectively. Then we sum these two masses $m_{H(\ell\ell)} + m_{H(\ell jj)}$. We choose the combination which yields a smaller value as the solution. We notice that this method reaches the highest percentage of correction combination up to 95%.

Therefore, in the following analysis, we will use the sum of invariant masses of Higgs bosons, i.e., the sixth method, to determine the combination and extract the relevant experimental observables at the hadron/detector level.

Another remarkable aspect is the missing energy, or more precisely the missing transverse momentum. In signal events, there are three neutrinos in total, which should have 9 degrees of freedom to determine the full phase space. But we can obtain have at most five constraints. So in principle, it is impossible to solve the kinematics at event-by-event level. Nevertheless, in the hypotheses of pair production, we can split the transverse missing momenta of each event into two parts. The first part will combine with the lepton pair to reconstruct the transverse mass of the first Higgs boson, and the second part should combine with the rest of the objects in the event to form that of the second Higgs boson. Below we will explore the variable m_{T2}.

B. The variable m_{T2}

The variable, m_T, is defined as the transverse mass of a mother particle, which has played a crucial role for the discovery of W boson [85]. The extended variable m_{T2} was introduced to extract the information of particle mass in pair production processes at hadron colliders [86,87] when the information of both the mass and longitudinal components of invisible particles is missing.

The original setup assumed the production of a pair of particles A_1 and A_2, then particles A_i decay into invisible particle B_i and visible particle C_i, for example: $pp \to A_1A_2, A_1 \to B_1C_1, A_2 \to B_2C_2$, where B_i particles denote invisible particles like neutrinos and neutralinos of the SUSY and C_i particles denote visible particles like leptons or jets of which the energies and momenta can be reconstructed by detectors. At hadron colliders, only the sum of transverse momentum of B_1 and B_2 which is denoted as $\not{E}_T$ can be reconstructed by assuming the energy conservation in the transverse directions. In experiments, the missing transverse momenta $\not{E}_T$ can be reconstructed by using the particle flow algorithm, for instance. Since the energy and longitudinal components are missing and in principle it is impossible to reconstruct the mass of m_A, we can define the transverse mass of particle A from the transverse momenta of the particles B and C: $M_T^2(P_T(B),P_T(C))=(E_T(B)+E_T(C))^2-(\vec{P}_T(B)+\vec{P}_T(C))^2$, where the transverse energy is defined as $E_T^2 = \vec{P}_T^2 + M^2$. There exists an inequality $M_T(B,C) \leq M(A)$.

In practice, to construct the variable m_{T2} we split the missing transverse momenta into two parts and to find the minimal of the maximal of reconstructed transverse mass:

$$m_{T2} = \min_{\vec{P}_{T1}+\vec{P}_{T2}=\not{E}_T} \{\max[m_T^2(\vec{P}_T(B_1), \vec{P}_T(C_1)), m_T^2(\vec{P}_T(B_2), \vec{P}_T(C_2))]\}.$$

For each event, the minimization is taken over all possible transverse momentum splitting. For a pair production event, the m_{T2} corresponds to find the solution where both reconstructed transverse masses from each decay chain are equal. Recently, there are more studies on the m_{T2} variable and its variants, interested readers can refer to [88–90] for more information.

Obviously, this variable can be generalized to the cases where either particles B or C are not a single particle then either A_1 or A_2 can decay into different final states. In the case at hand, the leptonic Higgs boson decays into $(l^{\pm}l^{\mp})(\nu\nu)$, and the semileptonic Higgs decays into $(l^{\pm}jj)(\nu)$. The invisible part of the leptonic Higgs contains two neutrinos and their invariant mass is unable to know. Considering that the variable m_{T2} is a monotonous increasing function on the m_{12}, for simplicity, we choose it as zero.

For the case at hand, after the splitting of missing transverse momenta, we can construct the transverse mass of the Higgs boson by using the m_{T2} code [91]. So the first part of the split $\not{E}_T$ should correspond to the combination of two neutrinos, and the second part of $\not{E}_T$ should correspond to a neutrino, so that the transverse mass of the Higgs boson can be constructed. The quantity is called the m_{T2} variable, which has utilized information of both the visible and invisible objects in an event. It is remarkable that this quantity is the most sensitive observable to distinguish

TABLE III. The efficiency of four crucial cuts are demonstrated. To appreciate the efficiency of each cut, we also provide the values of S/B and $S/\sqrt{B}$ after each cut.

	Signal H H	$t\bar{t}+W$	H W	W W W	$t\bar{t}H$	S/B	$S/\sqrt{B}$
No. after preselection	13.7	317.2	94.4	400.6	101.3	1.5×10^{-2}	0.45
$m_{jj}<80$ GeV	10.6	153.7	53.3	189.6	78.7	2.2×10^{-2}	0.49
$m_{H(\ell,jj)}<110$ GeV	9.6	70.6	27.8	78.2	54.8	4.2×10^{-2}	0.63
$m_{H(\ell\ell)}<55$ GeV	11.2	76.9	65.0	92.8	53.6	3.9×10^{-2}	0.66
$m_{T2}<110$ GeV	8.4	18.4	16.7	19.1	27.1	1.0×10^{-1}	0.93

signal and background, as shown in both Fig. 3(d) and Table III.

In Figure 3, we show the line shapes of signal and background events in terms of $m_{H(\ell\ell)}$, $\Delta R(\ell, jj)$, $m_{H(\ell jj)}$, and m_{T2}. From the line shapes, we introduce a one-dimensional cut for each of these observables. In Table III, we tabulate the efficiency of each cut. It is noticed the observable m_{T2} can have the best distinguishing power and the observable $m_{H(\ell\ell)}$ is the second powerful observable. From Table III, it is remarkable that the backgrounds from $t\bar{t}W$ and WWW can be heavily affected by this quantity since they are not pair production processes in nature. For the process HW, extra jets from initial state radiation should be used to balance the pair production hypothesis.

When we combine all of these cuts into a cut-based method, we arrive at the significance given in Table IV. After using the quantities extracted from our reconstruction procedure, we notice that the S/B can be improved by a factor 10 or so. Compared with the results given in Table I,

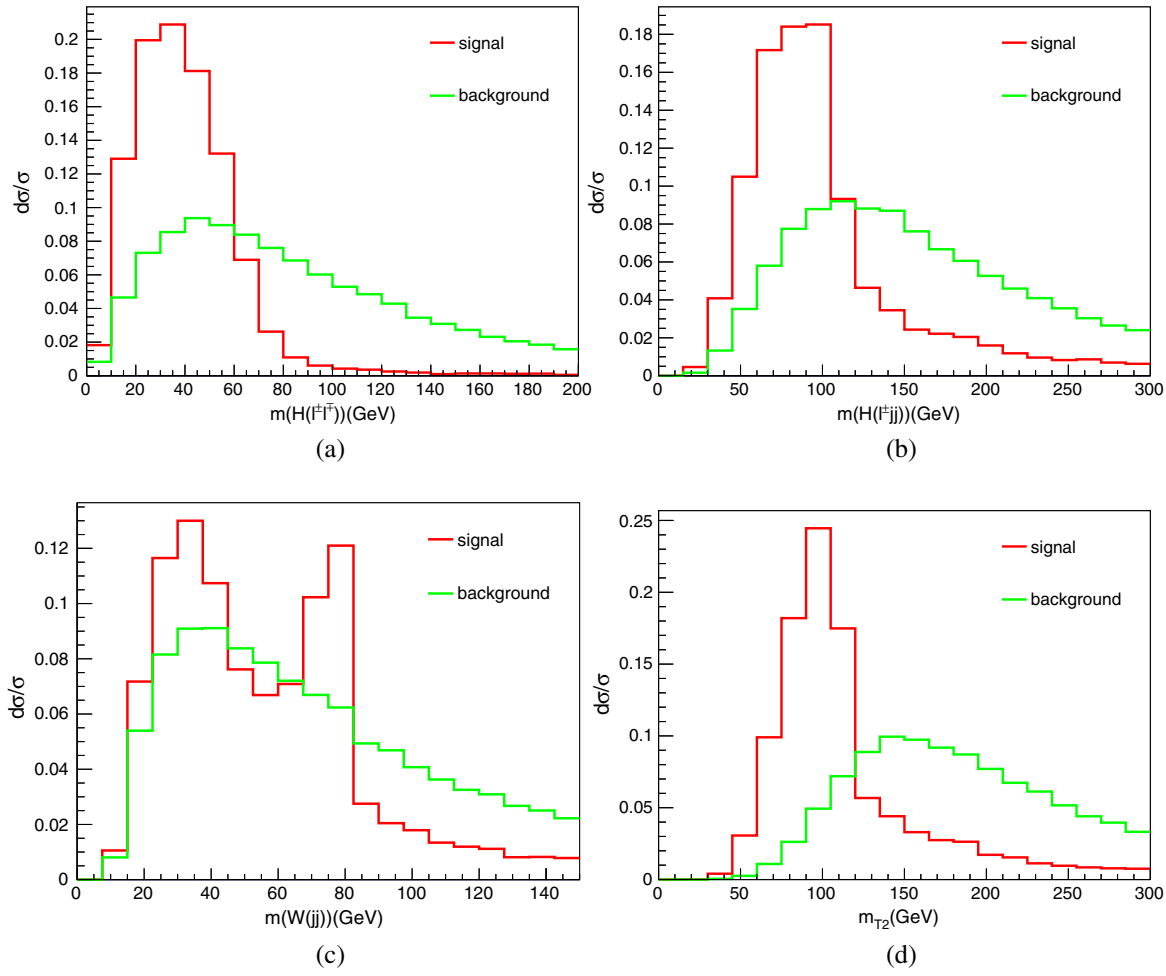

FIG. 3 (color online). Four crucial reconstructed kinematic observables at hadron level are demonstrated. (a) Mass of leptonic Higgs; (b) Mass of semileptonic Higgs; (c) The reconstructed W/W^*; (d) m_{T2}.

TABLE IV. The effects of each cut in the cut-based method are demonstrated in a sequential way. After all cuts, the values of S/B and $S/\sqrt{B}$ are provided.

	Signal H H	$t\bar{t}$+W	H W	W W W	$t\bar{t}$H
No. after preselection	13.7	317.2	94.4	400.6	101.3
$m_{T2} < 110$ GeV	8.4	18.4	16.7	19.1	27.1
$m_{H(\ell\ell)} < 55$ GeV	7.2	10.5	13.0	11.5	19.0
No. of jets $\leqq 4$	6.2	8.0	12.0	8.8	7.9
S/B			0.17		
$S/\sqrt{B}$			1.0		

we observe a big gain in both S/B and $S/\sqrt{B}$. The gain is mainly yielded by the success of suppression to the background processes $t\bar{t}W$ and WWW. In contrast, the suppression to the background HW is relatively limited due to the appearance of a real Higgs boson in the process and our reconstruction procedure can find the Higgs bosons in the events. For example, the cut $m_{H(\ell\ell)} < 55$ GeV has no serious effects to this background process. But, instead, the variables from the semileptonic Higgs can impose a significant suppression to this type of background.

IV. THE SENSITIVITY TO TRIPLE HIGGS COUPLING

A. The sensitivity to λ_3 at LHC 14 TeV with a 3 ab^{-1} data set

Considering that the number of signal events is few and the dimension of phase space of the final states is 24 (nine of them contributing to the missing energy in signal events) and most of the variables are correlated, we optimize these cuts and include more observables which are independent of those four observables in the cut-based method. We have included more kinematic observables in our analysis:

(i) The sum of transverse momenta of all objects used in the reconstruction procedure is considered, of

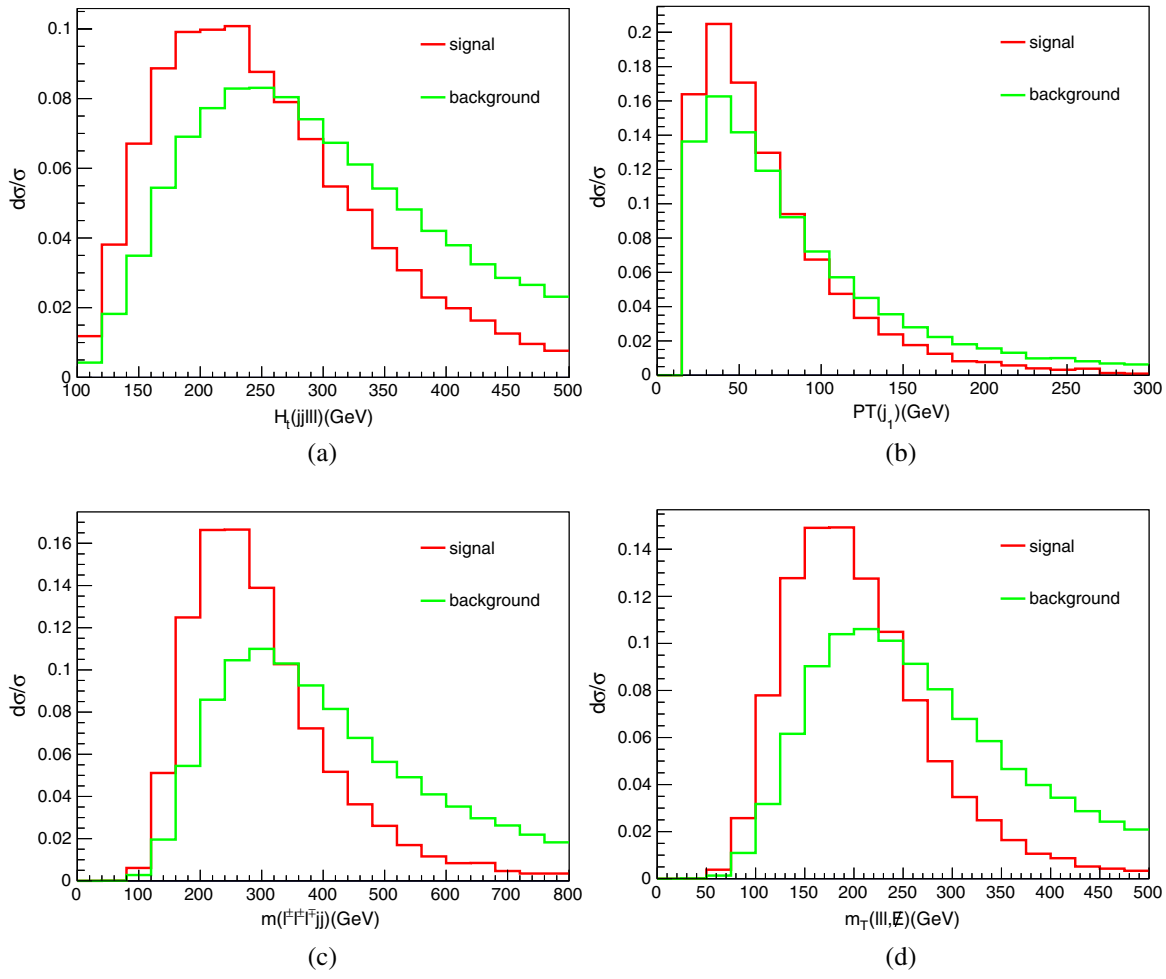

FIG. 4 (color online). We show more observables at hadron level used by the multivariable analyses. (a) P_t Sum of objects used for reconstruciton; (b) P_T of harder jet in the hadronic W boson; (c) Invariant mass of visible objects; (d) The transverse mass of leptons and E_T.

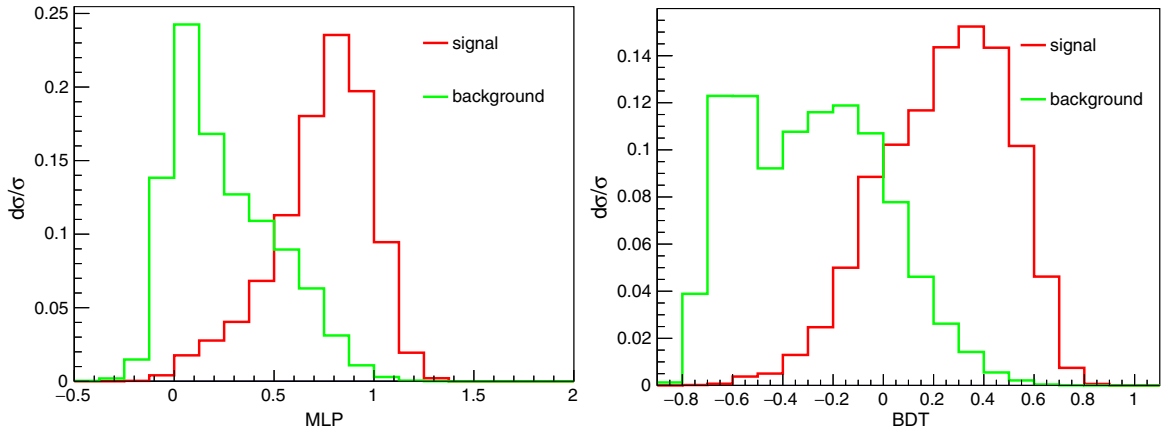

FIG. 5 (color online). The response of the discriminants to signal and background in two multivariable analyses, the MLP NN and BDT methods, is demonstrated. (a) MLP Neutral Network; (b) Boosted Decision Tree.

which the distribution of signal and background are shown in Fig. 4(a).

(ii) The transverse momenta of the harder jet used to reconstruct the hadronic W/W^* is taken into account and is shown in Fig. 4(b). Due to the existence of off-shell W bosons, the momentum is softer than the background events.

(iii) The invariant mass of all the visible objects (including three leptons and all jets) is presented in Fig. 4(c), we observe that the signal events typically have smaller values when compared with the background events.

(iv) The transverse mass obtained from the combined 4-momentum of three leptons and the missing transverse momentum is shown in Fig. 4(d).

We have also exploited other observables, like the transverse momenta of leptonic and semileptonic Higgs, the angular separation of two partially reconstructed Higgs bosons, the number of jets in each event, the ratio of missing energy over the visible energetic, etc.

We apply two multivariable analyses: one is BDT, the other is MLP neural network. The distributions of other useful observables are shown in Fig. 4. As demonstrated in Fig. 5, these observables are indeed helpful to discriminate signal and background events.

The results of multivariable analyses are presented in Table V and the distributions of discriminant response to signal and background are shown in Figure 6. We observe that the S/B can be improved by a factor 20 and the significance can reach up to 2.0 or so, which is very encouraging.

We plot the estimated sensitivity to λ_3 at LHC 14 TeV with a 3 ab^{-1} data set in Fig. 6(a). Although there are the large number of background events, we are capable to rule out the value of $\lambda_3 < -1.0$ and $\lambda_3 > 8.0$; while if λ_3 is

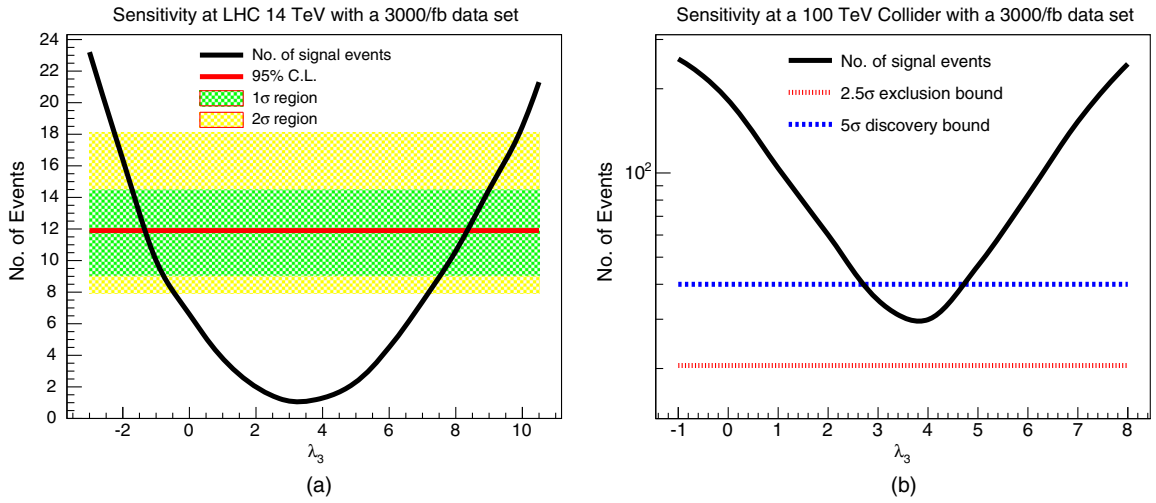

FIG. 6 (color online). The sensitivity to the triple couplings of Higgs boson, λ_3, at the LHC 14 TeV and a 100 TeV collider is shown. (a) Sensitivity at the LHC with a 3000 fb^{-1} data set; (b) Sensitivity at a 100 TeV collider with a 3000 fb^{-1} data set.

TABLE V. Comparison of significance among three analysis methods are shown.

	After preselection cuts	Cut-based method	MLP method $N_{NN} > 0.82$	BDT method $N_{\rm BDT} > 0.41$
No. of signal	13.7	6.2	5.7	3.8
No. of background	913.5	36.8	21.7	6.2
S/B	1.5×10^{-2}	1.7×10^{-1}	2.6×10^{-1}	6.2×10^{-1}
$S/\sqrt{B}$	0.45	1.0	1.2	1.5

within the range $-1.0 < \lambda_3 < 8$, it might be challenging to determine the value of λ_3 due to background fluctuations.

B. The sensitivity to λ_3 at a 100 TeV collider

We apply our analysis demonstrated in the last section to a 100 TeV collider. It is noticed that both the production rate of signal and background with top quarks enhanced by a factor 40 or more than 100. In Table VI, we tabulate the results obtained from the cut-based method and find that the significance can reach to 7.0.

When compared with the 14 TeV collider case, it is remarkable that the background $t\bar{t}H$ becomes the dominant one after all cuts. Here we have not applied any special variable to further suppress this type of background, we expect better results when these special variables of $t\bar{t}H$ are used. Another remarkable fact is that although the production rate of the background from $t\bar{t}t\bar{t}$ also enhances by a factor 200, simply by counting the number of jets can efficiently kill most of this type of background.

In Table. VII, we tabulate the optimized results. Similarly to the 14 TeV case, we notice that the significance can be improved by a factor of 3.5 or so and the ratio S/B can be improved by two orders.

The sensitivity of a 100 TeV collider to the triple coupling λ_3 is provided in Fig. 6(b). So a 100 TeV collider can exclude all values of λ_3 by simply using the three leptons mode considered in this paper. Here our multivariate analysis has been optimized for the SM, i.e., $\lambda_3 = 1$, all λ_3 out of the range [2.8, 4.5] can be discovered. Nonetheless, if we optimize our analysis to different λ_3, we notice that even for the minimal cross section case with $\lambda_3 = 3.6$ or so, the significance can reach to 5σ.

Since there is no doubt that the SM triple Higgs coupling can be discovered at a 100 TeV collider, below we are concerned with the issue of how well this coupling can be measured by just using the trilepton mode considered in this paper. To address this issue, we use the invariant mass of three leptons to perform a χ^2 analysis. The distributions of this variable after the preselection cuts and the multivariate analysis are shown in Fig. 7. We have deliberately chosen three different values of λ_3 to demonstrate the differences in magnitudes and shapes. Since all cuts are optimized to the SM case, one can perceive the signal shapes of the cases $\lambda_3 = -2$ and $\lambda_3 = 5$ have been greatly changed by the MVA filter.

Below we address the issue of how well the value of λ_3 can be determined. By using the method described in Refs. [61,92], we use ten bins to perform a χ^2 analysis on the distributions of the invariant mass of three leptons. The expression for χ^2 is given by [92]

$$\chi^2(\lambda_3) = \sum_{i=1}^{n_D} \frac{(N_i - fN_i^0)^2}{fN_i^0} + (n_D - 1), \qquad (2)$$

TABLE VI. The effects of each cut in the cut-based method are demonstrated in a sequential way for a 100 TeV collider. After all cuts, the values of S/B and $S/\sqrt{B}$ are provided.

	Signal H H	$t\bar{t} + W$	H W	W W W	$t\bar{t}H$	$t\bar{t}t\bar{t}$
No. after preselection	416.8	4392.3	716.1	4384.1	5045.9	263.48
$m_{T2} < 110$ GeV	234.3	234.6	116.8	125.4	1152.9	26.8
$m_{H(\ell\ell)} < 55$ GeV	202.3	133.9	94.8	71.6	811.6	15.5
No. of jets $\leq$4	160.0	81.8	82.4	53.5	304.9	1.0
S/B			0.31			
$S/\sqrt{B}$			7.0			

TABLE VII. Comparison of significance among three analysis methods in a 100 TeV collider are shown.

	After preselection cuts	Cut-based method	MLP method $N_{NN} > 0.94$	BDT method $N_{\rm BDT} > 0.22$
No. of signal	416.8	160.0	80.4	104.0
No. of background	14801.8	523.6	107.3	67.1
S/B	2.8×10^{-2}	3.1×10^{-1}	7.5×10^{-1}	1.5
$S/\sqrt{B}$	3.43	7.0	7.8	12.7

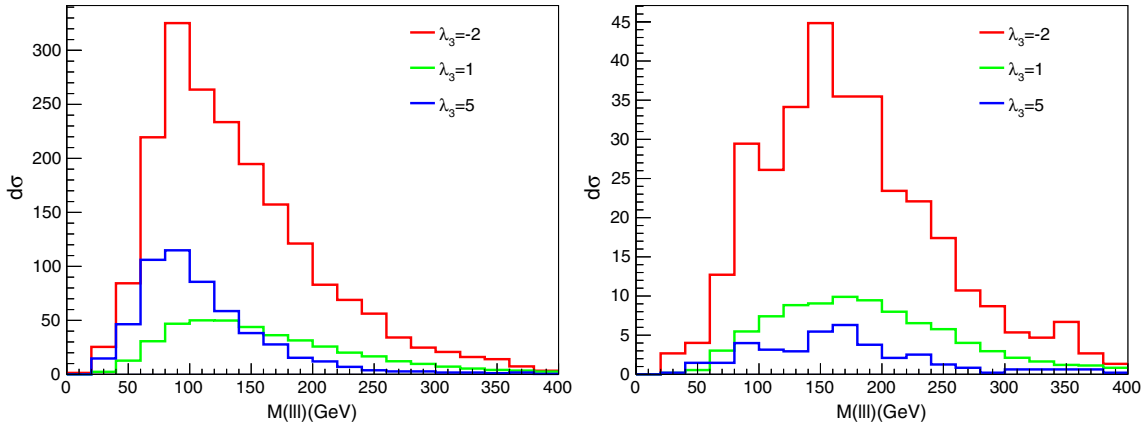

FIG. 7 (color online). The distributions of the invariant mass of three leptons after preselection and after MVA cut are demonstrated, where the background events have been neglected. Three different values of λ_3 are chosen to show how the triple Higgs coupling can affect the magnitudes and shapes. (a) Three leptons mass after preselection; (b) Three lepton mass after MVA cut.

where n_D denotes the number of bins, and N_i is the number of events which include both the signal and background after cuts. Obviously N_i is dependent upon the triple Higgs coupling parameter λ_3. N_i^0 means the number of events in the SM in the ith bin after cuts, here the SM means $\lambda_3 = 1$. Here the quantity f encodes the uncertainty in the normalization of the SM cross section within the allowed range, which is determined by minimizing χ^2:

$$f = \begin{cases} (1+\Delta N)^{-1} & \text{for } \bar{f} < (1+\Delta N)^{-1}, \\ \bar{f} & \text{for } (1+\Delta N)^{-1} < \bar{f} < 1+\Delta N, \\ 1+\Delta f & \text{for } \bar{f} > 1+\Delta n, \end{cases}$$

where ΔN is taken as 10% of the SM cross section (including both the signal and background after all cuts). The parameter $\bar{f}$ is defined as

$$\bar{f}^2 = \sum_{i=1}^{n_D} \frac{N_i^2}{N_i^0} \Big/ \left(\sum_{i=1}^{n_D} N_i^0 \right).$$

The results are presented in Fig. 8 where the common term $n_D - 1$ has been omitted. There are two comments in order:

(i) In the Fig. 8(a), we observe that a 100 TeV collider can distinguish the two cases $\lambda_3 = 1$ and $\lambda_3 = 6.3$, although total cross sections of these two cases are equal. The difference in the line shapes of the invariant mass of three leptons is sufficient to separate them from each other.

To appreciate the underlying reason why these two cases are separable, at leading order, we can represent the differential cross section in the following form as

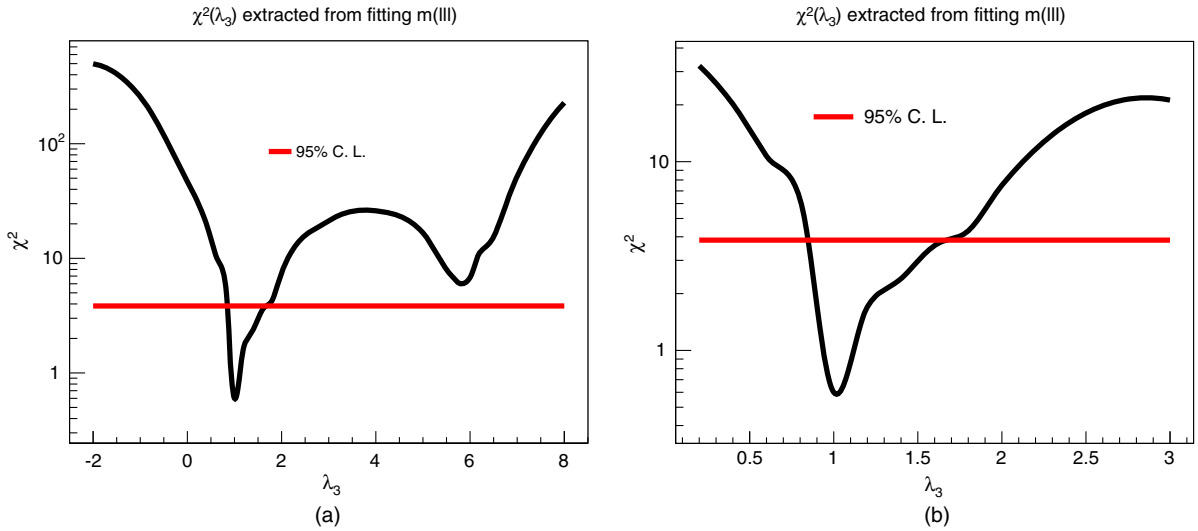

FIG. 8 (color online). The χ^2 varying with λ_3 at a 100 TeV collider with a data set 3000 fb^{-1} is shown. (a) χ^2 varying with λ_3; (b) Fine structure of χ^2 near $\lambda_3 = 1$.

$$\frac{d^2\sigma}{ds d\cos\theta} = (\lambda_3 C_\triangle + C_\square)^2 + D_\square^2, \quad (3)$$

where the $C_\triangle$ and $C_\square$ are $S=0$ form factors and $D_\square$ is $S=2$ form factor, which are dependent upon s and $\cos\theta$ and their exact expressions at leading order can be found in [93]. In terms of this form, total cross section can be expressed as

$$\bar{\sigma} = \lambda_3^2 \overline{C_\triangle^2} + 2\lambda_3 \overline{C_\triangle C_\square} + \overline{C_\square^2 + D_\square^2}, \quad (4)$$

where all overlined quantities, like $\overline{C_\triangle^2}$, $\overline{C_\triangle C_\square}$, and $\overline{C_\square^2 + D_\square^2}$, denote the integrated values, which are just numbers. When total cross section is fixed as $\bar{\sigma}$ by experimental measurements, there are two solutions of λ_3 which can yield the same total cross section. These two solutions can be expressed below as

$$\lambda_3^{\pm} = \frac{\overline{C_\triangle C_\square} \pm \sqrt{(\bar{\sigma} - \overline{C_\square^2 - D_\square^2})\overline{C_\triangle^2} - \overline{C_\triangle C_\square}^2}}{\overline{C_\triangle^2}}. \quad (5)$$

From these two solutions, the difference of differential cross section between them can be expressed as

$$\frac{d^2\sigma^+}{ds d\cos\theta} - \frac{d^2\sigma^-}{ds d\cos\theta} = 2(\lambda_3^- - \lambda_3^+) C_\triangle \left(C_\square - \frac{\overline{C_\triangle C_\square}}{\overline{C_\triangle^2}} C_\triangle \right). \quad (6)$$

It is noticed that two form factors, i.e., $C_\triangle$ and $C_\square$, can completely determine the difference of line shapes of these two cases.

(ii) In the Fig. 8(b), we observe that by using the χ^2 fit of the invariant mass of three leptons, the value of λ_3 can be determined as $1^{+0.6}_{-0.3}$ in the 95% confidence level, which is wider than the value $1^{+0.2}_{-0.1}$ or so when only the statistic accuracy is taken into account. But if the total luminosity can reach to 30 ab^{-1}, it is possible to reach this precision or better. This result is comparable to the precision which might be achieved from both the signals of the $b\bar{b}\gamma\gamma$ final state and those of $b\bar{b}\gamma\gamma$ with a hard jet [94].

Since observables constructed from leptons are expected to be more robust than those constructed from jets due to the contamination of underlying events and pileup of high luminosity run at future colliders, so we have used the invariant mass of three leptons to perform the χ^2 fit. We can use the line shape of the transverse momenta of leptonic Higgs, the invariant of leptonic Higgs, etc., to perform alternative χ^2 analysis. It is noticed that they can yield similar results.

V. DISCUSSION AND CONCLUSION

In this paper, we have considered the feasibility of the $3\ell 2j + \not{E}$ mode to discover the signal of Higgs pair production at the LHC and a 100 TeV collider. We have proposed a partial reconstruction procedure to reconstruct two Higgs bosons in the final state and have examined the m_{T2} observable in the hypothesis of pair production to discriminate the signal and background events. Although the production rate of signal events at the LHC 14 TeV 3000 fb^{-1} is small, we have found that this mode can yield a significance around 1.5 or so. For a 100 TeV collider with the same integrated luminosity, we noticed this mode can be used to determine the λ_3 and triple coupling of the Higgs boson of the standard model can be determined into the range $1^{+0.6}_{-0.3}$. If the total integrated luminosity is 30 ab^{-1}, we estimated that it is possible to achieve $1^{+0.2}_{-0.1}$.

At our hadron level simulation, in order to take more signal into account, we have deliberately chosen $\Delta R(\ell) \geq 0.2$ to find isolated leptons; after having found these objects, we cluster the rest of the particles and energy into

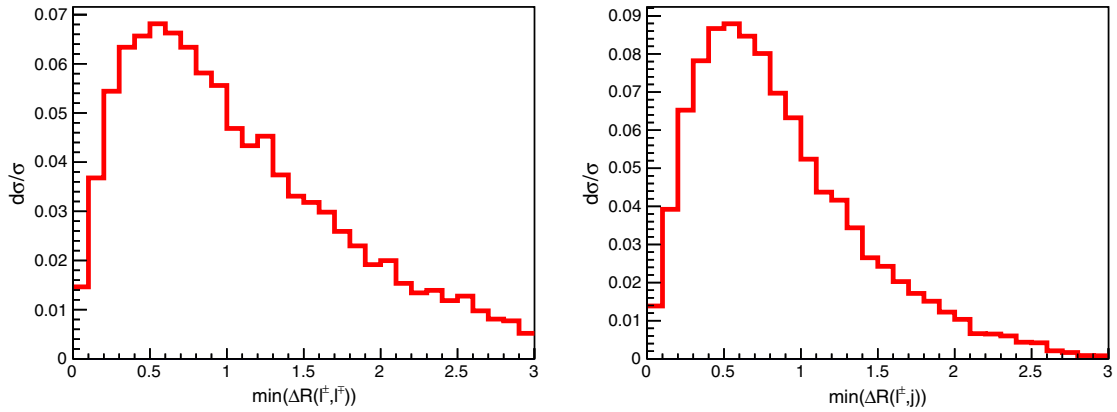

FIG. 9 (color online). For the signal events at the hadron level, we show the minimal angle separation between two leptons (the left panel) and the minimal angle separation between a lepton and a jet (the right panel) here.

jets. We notice that the angular separation cuts between leptons and that between a lepton and a jet can affect the selection efficiency of signal events to a quite considerable degree. Therefore, we provide the distributions of $\Delta R^{\min}(\ell,\ell)$ and $\Delta R^{\min}(\ell,j)$ in Fig. 9.

In this paper, we have used the lepton isolation criteria $\Delta R(\ell) = 0.2$, which is possible when the fine granularity of tracker detector and electromagnetic calorimeter are taken into account. By changing this condition to $\Delta R(\ell) = 0.3$, we observe that the signal loss is around 10%. When we demand $R^{\min}(\ell, j) \leq 0.4$, we notice that the signal loss is around 15%.

We have not included more detailed detector effects, like the pileup effects which may mitigate the reconstruction of two soft jets coming from the off-shell W decay. For a more realistic 100 TeV collision study, the pileup effects can be a serious issue [95] due to the fact that we need to identify two jets in the signal event, which deserves our future careful study.

We have used the B veto and have assumed B tagging efficiency as 0.6. If the B tagging efficiency is assumed to be 0.7 and more background events from $t\bar{t}W$ can be better rejected, then we expect a better realistic significance. Besides, information of color flow of two jets from W/W^*, which are color singlet objects, can be used to determine the right combination and may provide further improvement. Considering these potential further improvements for this mode, and in contrast to the contamination of pileup effects and underlying events which might mitigate the modes with B jets in the final states for the $bb\gamma\gamma$ mode [96], we believe this mode might be robust and promising and should be seriously considered by experimenters.

We can extend this paper to study the same-sign dilepton modes of the Higgs pair production at both the context of the LHC and a 100 TeV collider. In a 100 TeV collider, the production rate of the Higgs pair can be quite significant, we can extend the partial reconstruction method and analysis demonstrated here to the four-leptonic mode of Higgs pair production, which should be clean and robust against the contamination of underlying events and pileup effects.

ACKNOWLEDGMENTS

This work is supported by the Natural Science Foundation of China under Grants No. 11175251, No. 11205008, No. 11305179, and No. 11475180.

[1] G. Aad *et al.* (ATLAS Collaboration), Observation of a new particle in the search for the Standard Model Higgs boson with the ATLAS detector at the LHC, Phys. Lett. B **716**, 1 (2012).

[2] S. Chatrchyan *et al.* (CMS Collaboration), Observation of a new boson at a mass of 125 GeV with the CMS experiment at the LHC, Phys. Lett. B **716**, 30 (2012).

[3] H. Baer, T. Barklow, K. Fujii, Y. Gao, A. Hoang, S. Kanemura, J. List, H. E. Logan *et al.*, The International Linear Collider technical design report—volume 2: Physics, arXiv:1306.6352.

[4] S. Dawson, A. Gritsan, H. Logan, J. Qian, C. Tully, R. Van Kooten, A. Ajaib, A. Anastassov *et al.*, Working Group report: Higgs boson, arXiv:1310.8361.

[5] R. Brock, M. E. Peskin, K. Agashe, M. Artuso, J. Campbell, S. Dawson, R. Erbacher, C. Gerber *et al.*, Planning the future of U.S. particle physics (Snowmass 2013): Chapter 3: Energy frontier, arXiv:1401.6081.

[6] W. Yao, Studies of measuring Higgs self-coupling with $HH \to b\bar{b}\gamma\gamma$ at the future hadron colliders, arXiv:1308.6302.

[7] O. J. P. Eboli, G. C. Marques, S. F. Novaes, and A. A. Natale, Twin Higgs boson production, Phys. Lett. B **197**, 269 (1987).

[8] W. Y. Keung, Double Higgs from $W - W$ fusion, Mod. Phys. Lett. A **02**, 765 (1987).

[9] D. A. Dicus, K. J. Kallianpur, and S. S. D. Willenbrock, Higgs boson pair production in the effective W approximation, Phys. Lett. B **200**, 187 (1988).

[10] T. Plehn, M. Spira, and P. M. Zerwas, Pair production of neutral Higgs particles in gluon-gluon collisions, Nucl. Phys. **B479**, 46 (1996); **531**, 655(E) (1998).

[11] S. Dawson, S. Dittmaier, and M. Spira, Neutral Higgs boson pair production at hadron colliders: QCD corrections, Phys. Rev. D **58**, 115012 (1998).

[12] D. de Florian and J. Mazzitelli, Higgs Boson Pair Production at Next-to-Next-to-Leading Order in QCD, Phys. Rev. Lett. **111**, 201801 (2013).

[13] J. Grigo, J. Hoff, K. Melnikov, and M. Steinhauser, On the Higgs boson pair production at the LHC, Nucl. Phys. **B875**, 1 (2013).

[14] L. Liu-Sheng, Z. Ren-You, M. Wen-Gan, G. Lei, L. Wei-Hua, and L. Xiao-Zhou, NNLO QCD corrections to Higgs pair production via vector boson fusion at hadron colliders, Phys. Rev. D **89**, 073001 (2014).

[15] E. Asakawa, D. Harada, S. Kanemura, Y. Okada, and K. Tsumura, Higgs boson pair production in new physics models at hadron, lepton, and photon colliders, Phys. Rev. D **82**, 115002 (2010).

[16] G. D. Kribs and A. Martin, Enhanced di-Higgs production through light colored scalars, Phys. Rev. D **86**, 095023 (2012).

[17] J. M. No and M. Ramsey-Musolf, Probing the Higgs portal at the LHC through resonant di-Higgs production, Phys. Rev. D **89**, 095031 (2014).

[18] J. Liu, X. P. Wang, and S. H. Zhu, Discovering extra Higgs boson via pair production of the SM-like Higgs bosons, arXiv:1310.3634.

[19] Z. Heng, L. Shang, Y. Zhang, and J. Zhu, Pair production of 125 GeV Higgs boson in the SM extension with color-octet scalars at the LHC, J. High Energy Phys. 02 (2014) 083.
[20] J. Cao, D. Li, L. Shang, P. Wu, and Y. Zhang, Exploring the Higgs sector of a most natural NMSSM and its prediction on Higgs pair production at the LHC, J. High Energy Phys. 12 (2014) 026.
[21] A. Doff and A. A. Natale, Scalar bosons in minimal and ultraminimal technicolor: Masses, trilinear couplings and widths, Phys. Rev. D **81**, 095014 (2010).
[22] A. Belyaev, M. Drees, O. J. P. Eboli, J. K. Mizukoshi, and S. F. Novaes, Supersymmetric Higgs pair production at hadron colliders, Phys. Rev. D **60**, 075008 (1999).
[23] A. Belyaev, M. Drees, and J. K. Mizukoshi, Supersymmetric Higgs boson pair production: Discovery prospects at hadron colliders, Eur. Phys. J. C **17**, 337 (2000).
[24] J. Cao, Z. Heng, L. Shang, P. Wan, and J. M. Yang, Pair production of a 125 GeV Higgs boson in MSSM and NMSSM at the LHC, J. High Energy Phys. 04 (2013) 134.
[25] M. Moretti, S. Moretti, F. Piccinini, R. Pittau, and A. D. Polosa, Higgs boson self-couplings at the LHC as a probe of extended Higgs sectors, J. High Energy Phys. 02 (2005) 024.
[26] Z. Z. Xianyu, J. Ren, and H. J. He, Gravitational interaction of Higgs boson and weak boson scattering, Phys. Rev. D **88**, 096013 (2013).
[27] J. Ren, Z. Z. Xianyu, and H. J. He, Higgs gravitational interaction, weak boson scattering, and Higgs inflation in Jordan and Einstein frames, J. Cosmol. Astropart. Phys. 06 (2014) 032.
[28] G. F. Giudice, C. Grojean, A. Pomarol, and R. Rattazzi, The strongly-interacting light Higgs, J. High Energy Phys. 06 (2007) 045.
[29] F. Goertz, A. Papaefstathiou, L. L. Yang, and J. Zurita, Higgs boson pair production in the D = 6 extension of the SM, J. High Energy Phys. 04 (2015) 167.
[30] R. Frederix, S. Frixione, V. Hirschi, F. Maltoni, O. Mattelaer, P. Torrielli, E. Vryonidou, and M. Zaro, Higgs pair production at the LHC with NLO and parton-shower effects, Phys. Lett. B **732**, 142 (2014).
[31] J. Baglio, A. Djouadi, R. Grber, M. M. Mhlleitner, J. Quevillon, and M. Spira, The measurement of the Higgs self-coupling at the LHC: Theoretical status, J. High Energy Phys. 04 (2013) 151.
[32] F. Maltoni, E. Vryonidou, and M. Zaro, Top-quark mass effects in double and triple Higgs production in gluon-gluon fusion at NLO, J. High Energy Phys. 11 (2014) 079.
[33] M. Slawinska, W. van den Wollenberg, B. van Eijk, and S. Bentvelsen, Phenomenology of the trilinear Higgs coupling at proton-proton colliders, arXiv:1408.5010.
[34] D. Y. Shao, C. S. Li, H. T. Li, and J. Wang, Threshold resummation effects in Higgs boson pair production at the LHC, J. High Energy Phys. 07 (2013) 169.
[35] C. S. Li, H. T. Li, and D. Y. Shao, Some recent theoretical progress in Higgs boson and top quark physics at hadron colliders, Chin. Sci. Bull. **59**, 3709 (2014).
[36] P. A. Baikov, K. G. Chetyrkin, and J. H. Kuhn, Scalar Correlator at $O(\alpha_S^4)$, Higgs Decay into b-quarks and Bounds on the Light Quark Masses, Phys. Rev. Lett. **96**, 012003 (2006).
[37] P. A. Baikov and K. G. Chetyrkin, Top Quark Mediated Higgs Boson Decay into Hadrons to Order α_s^5, Phys. Rev. Lett. **97**, 061803 (2006).
[38] M. Schreck and M. Steinhauser, Higgs decay to gluons at NNLO, Phys. Lett. B **655**, 148 (2007).
[39] G. Passarino, C. Sturm, and S. Uccirati, Complete two-loop corrections to $H \to \gamma\gamma$, Phys. Lett. B **655**, 298 (2007).
[40] P. Maierhfer and P. Marquard, Complete three-loop QCD corrections to the decay $H \to \gamma\gamma$, Phys. Lett. B **721**, 131 (2013).
[41] M. Spira, A. Djouadi, and P. M. Zerwas, QCD corrections to the H Z gamma coupling, Phys. Lett. B **276**, 350 (1992).
[42] A. Bredenstein, A. Denner, S. Dittmaier, and M. M. Weber, Precise predictions for the Higgs-boson decay $H \to WW/ZZ \to 4$ leptons, Phys. Rev. D **74**, 013004 (2006).
[43] A. Bredenstein, A. Denner, S. Dittmaier, and M. M. Weber, Radiative corrections to the semileptonic and hadronic Higgs-boson decays $H \to WW/ZZ \to 4$ fermions, J. High Energy Phys. 02 (2007) 080.
[44] A. Bredenstein, A. Denner, S. Dittmaier, and M. M. Weber, Precision calculations for $H \to WW/ZZ \to 4$ fermions with PROPHECY4f, arXiv:0708.4123.
[45] A. Djouadi, The anatomy of electro-weak symmetry breaking. I: The Higgs boson in the standard model, Phys. Rep. **457**, 1 (2008).
[46] A. Djouadi, The anatomy of electro-weak symmetry breaking. II. The Higgs bosons in the minimal supersymmetric model, Phys. Rep. **459**, 1 (2008).
[47] S. Dittmaier *et al.* (LHC Higgs Cross Section Working Group Collaboration), Handbook of LHC Higgs cross sections: 1. Inclusive observables, arXiv:1101.0593.
[48] S. Dittmaier, S. Dittmaier, C. Mariotti, G. Passarino, R. Tanaka, S. Alekhin, J. Alwall, E. A. Bagnaschi *et al.*, Handbook of LHC Higgs cross sections: 2. Differential distributions, arXiv:1201.3084.
[49] S. Heinemeyer *et al.* (LHC Higgs Cross Section Working Group Collaboration), Handbook of LHC Higgs cross sections: 3. Higgs properties, arXiv:1307.1347.
[50] J. Baglio, A theoretical status of the triple Higgs coupling studies at the LHC, arXiv:1408.6066.
[51] U. Baur, T. Plehn, and D. L. Rainwater, Probing the Higgs self-coupling at hadron colliders using rare decays, Phys. Rev. D **69**, 053004 (2004).
[52] CMS Collaboration, Search for the resonant production of two Higgs bosons in the final state with two photons and two bottom quarks, Report No. CMS-PAS-HIG-13-032.
[53] U. Baur, T. Plehn, and D. L. Rainwater, Examining the Higgs boson potential at lepton and hadron colliders: A comparative analysis, Phys. Rev. D **68**, 033001 (2003).
[54] M. J. Dolan, C. Englert, and M. Spannowsky, Higgs self-coupling measurements at the LHC, J. High Energy Phys. 10 (2012) 112.
[55] A. Papaefstathiou, L. L. Yang, and J. Zurita, Higgs boson pair production at the LHC in the $b\bar{b}W^+W^-$ channel, Phys. Rev. D **87**, 011301 (2013).
[56] D. E. Ferreira de Lima, A. Papaefstathiou, and M. Spannowsky, Standard model Higgs boson pair production in the $(b\bar{b})(b\bar{b})$ final state, J. High Energy Phys. 08 (2014) 030.

[57] V. Khachatryan *et al.* (CMS Collaboration), Search for resonant pair production of Higgs bosons decaying to two bottom quark-antiquark pairs in proton-proton collisions at 8 TeV, arXiv:1503.04114.

[58] M. J. Dolan, C. Englert, N. Greiner, and M. Spannowsky, Further on Up the Road: $hhjj$ Production at the LHC, Phys. Rev. Lett. **112**, 101802 (2014).

[59] T. Liu and H. Zhang, Measuring Di-Higgs Physics via the $t\bar{t}hh \to t\bar{t}b\bar{b}b\bar{b}$ Channel, arXiv:1410.1855

[60] U. Baur, T. Plehn, and D. L. Rainwater, Measuring the Higgs Boson Self-Coupling at the LHC and Finite Top Mass Matrix Elements, Phys. Rev. Lett. **89**, 151801 (2002).

[61] U. Baur, T. Plehn, and D. L. Rainwater, Determining the Higgs boson self-coupling at hadron colliders, Phys. Rev. D **67**, 033003 (2003).

[62] F. Goertz, A. Papaefstathiou, L. L. Yang, and J. Zurita, Higgs Boson self-coupling measurements using ratios of cross sections, J. High Energy Phys. 06 (2013) 016.

[63] R. Pittau, Status of MadLoop/aMC@NLO, arXiv:1202.5781.

[64] G. Cullen, H. van Deurzen, N. Greiner, G. Heinrich, G. Luisoni, P. Mastrolia, E. Mirabella, G. Ossola *et al.*, G*OSAM*-2.0: A tool for automated one-loop calculations within the Standard Model and beyond, Eur. Phys. J. C **74**, 3001 (2014).

[65] T. Hahn and M. Perez-Victoria, Automatized one loop calculations in four-dimensions and D-dimensions, Comput. Phys. Commun. **118**, 153 (1999).

[66] K. Arnold, M. Bahr, G. Bozzi, F. Campanario, C. Englert, T. Figy, N. Greiner, C. Hackstein *et al.*, VBFNLO: A parton level Monte Carlo for processes with electroweak bosons, Comput. Phys. Commun. **180**, 1661 (2009).

[67] K. Arnold, J. Bellm, G. Bozzi, M. Brieg, F. Campanario, C. Englert, B. Feigl, J. Frank *et al.*, VBFNLO: A parton level Monte Carlo for processes with electroweak bosons—Manual for version 2.5.0, arXiv:1107.4038.

[68] J. Baglio, J. Bellm, F. Campanario, B. Feigl, J. Frank, T. Figy, M. Kerner, L. D. Ninh *et al.*, Release note—VBFNLO 2.7.0, arXiv:1404.3940.

[69] J. Pumplin, D. R. Stump, J. Huston, H. L. Lai, P. M. Nadolsky, and W. K. Tung, New generation of parton distributions with uncertainties from global QCD analysis, J. High Energy Phys. 07 (2002) 012.

[70] Q. Li, Q. S. Yan, and X. Zhao, Higgs pair production: Improved description by matrix element matching, Phys. Rev. D **89**, 033015 (2014).

[71] J. Alwall, M. Herquet, F. Maltoni, O. Mattelaer, and T. Stelzer, MadGraph 5: Going beyond, J. High Energy Phys. 06 (2011) 128.

[72] T. Sjostrand, S. Mrenna, and P. Z. Skands, PYTHIA 6.4 physics and manual, J. High Energy Phys. 05 (2006) 026.

[73] M. L. Mangano, M. Moretti, F. Piccinini, and M. Treccani, Matching matrix elements and shower evolution for top-quark production in hadronic collisions, J. High Energy Phys. 01 (2007) 013.

[74] M. Cacciari, G. P. Salam, and G. Soyez, FastJet user manual, Eur. Phys. J. C **72**, 1896 (2012).

[75] M. Cacciari, G. P. Salam, and G. Soyez, The anti-k(t) jet clustering algorithm, J. High Energy Phys. 04 (2008) 063.

[76] ATLAS, Detector and physics performance technical design report, Vol. I, Report No. CERN/LHCC-99-14.

[77] CMS, Technical design report, detector performance and software, Vol. I, Report No. CERN-LHCC-2006-001.

[78] G. Ferrera, M. Grazzini, and F. Tramontano, Associated WH Production at Hadron Colliders: A Fully Exclusive QCD Calculation at NNLO, Phys. Rev. Lett. **107**, 152003 (2011).

[79] T. Binoth, G. Ossola, C. G. Papadopoulos, and R. Pittau, NLO QCD corrections to tri-boson production, J. High Energy Phys. 06 (2008) 082.

[80] J. M. Campbell and R. K. Ellis, $t\bar{t}W^{\pm}$ production and decay at NLO, J. High Energy Phys. 07 (2012) 052.

[81] W. Beenakker, S. Dittmaier, M. Kramer, B. Plumper, M. Spira, and P. M. Zerwas, NLO QCD corrections to $t\bar{t}H$ production in hadron collisions, Nucl. Phys. **B653**, 151 (2003).

[82] J. M. Campbell and R. K. Ellis, An update on vector boson pair production at hadron colliders, Phys. Rev. D **60**, 113006 (1999).

[83] Q. H. Cao and C. R. Chen, Resummation effects in the search of SM Higgs boson at hadron colliders, Phys. Rev. D **76**, 073006 (2007).

[84] J. Alwall, P. Demin, S. de Visscher, R. Frederix, M. Herquet, F. Maltoni, T. Plehn, D. L. Rainwater, and T. Stelzer, MadGraph/MadEvent v4: The New Web generation, J. High Energy Phys. 09 (2007) 028.

[85] J. Smith, W. L. van Neerven, and J. A. M. Vermaseren, The Transverse Mass and Width of the W boson, Phys. Rev. Lett. **50**, 1738 (1983).

[86] C. G. Lester and D. J. Summers, Measuring masses of semi-invisibly decaying particles pair produced at hadron colliders, Phys. Lett. B **463**, 99 (1999).

[87] A. Barr, C. Lester, and P. Stephens, m(T2): The truth behind the glamour, J. Phys. G **29**, 2343 (2003).

[88] A. J. Barr and C. G. Lester, A review of the mass measurement techniques proposed for the Large Hadron Collider, J. Phys. G **37**, 123001 (2010).

[89] A. J. Barr, T. J. Khoo, P. Konar, K. Kong, C. G. Lester, K. T. Matchev, and M. Park, Guide to transverse projections and mass-constraining variables, Phys. Rev. D **84**, 095031 (2011).

[90] W. S. Cho, J. S. Gainer, D. Kim, K. T. Matchev, F. Moortgat, L. Pape, and M. Park, On-shell constrained M_2 variables with applications to mass measurements and topology disambiguation, J. High Energy Phys. 08 (2014) 070.

[91] A. J. Barr and C. G. Lester, Oxbridge Stransverse Mass Library, http://www.hep.phy.cam.ac.uk/lester/mt2/index.html.

[92] U. Baur and E. L. Berger, Probing the weak boson sector in $Z\gamma$ production at hadron colliders, Phys. Rev. D **47**, 4889 (1993).

[93] E. W. N. Glover and J. J. van der Bij, Higgs boson pair production via gluon fusion, Nucl. Phys. **B309**, 282 (1988).

[94] A. J. Barr, M. J. Dolan, C. Englert, D. E. Ferreira de Lima, and M. Spannowsky, Higgs self-coupling measurements at a 100 TeV hadron collider, J. High Energy Phys. 02 (2015) 016.

[95] J. de Favereau, C. Delaere, P. Demin, A. Giammanco, V. Lematre, A. Mertens, and M. Selvaggi, DELPHES 3, A modular framework for fast simulation of a generic collider experiment, J. High Energy Phys. 02 (2014) 057.

[96] ATLAS Collaboration, Prospects for measuring Higgs H → $\gamma\gamma$ H → bb pair production in the channel using the ATLAS detector at the HL-LHC, Report No. ATL-PHYS-PUB-2014-019.